Impact of Optimized Flow Pattern on Pollutant Removal and Biogas Production Rate Using Wastewater Anaerobic Fermentation

Ruyi Huang,[a,b,c] Zili Mei,[b] Yan Long,[b] Xia Xiong,[b] Jun Wang,[a] Ting Guo,[c] Tao Luo,[a,b] and Enshen Long [a,*]

This paper introduces a new-type of antigravity mixing method, which was applied in the biogas production process, using organic wastewater fermentation. It was found that the digesters with two designs, a high-position, centralized pressure outlet and a high-position, dispersed pressure outlets, both lead to an increase in biogas production rates by 89% and 125%, respectively. The biogas production peak appeared 1 day and 7 days earlier, and the COD removal rates were raised by 27% and 42%, respectively. The results indicated that the optimized flow field had a significant impact. This work also explains the mechanism of flow field optimization using computational fluid dynamics (CFD) software for the simulation of the flow field form in the hydraulic mixing.

Keywords: Biogas; Mixing; Wastewater; Anaerobic digestion; CFD

Contact information: a: College of Architecture and Environment, Sichuan University, Chengdu 610065 China; b: Biogas Institute of Ministry of Agriculture (BIOMA), P.R. China, Chengdu 610041 China; c: Rural Energy Office of Sichuan Province, Chengdu 610041 China;
**Corresponding author: longes2@163.com*

ACRONYMS AND UNITS

COD —— chemical oxygen demand
CFD —— computational fluid dynamics
TS —— total solids
pH —— hydrogen ion concentration (negative log, base ten)
NH_3-N —— ammonia nitrogen
L —— litre
mm —— millimetre
Pa —— Pascal
s —— second
kg/m³ —— kilogram/ cubic metre
mg —— milligram
ρ —— mass
u_i —— vector velocity
τ_{ij} —— shear stress

INTRODUCTION

The production of biogas requires an operative engineering technology in the field of renewable energy and environmental protection that employs a simple anaerobic fermentation process to convert waste, including animal manure, crop straw, and organic wastewater, into methane. Although inorganic pollutants cannot be removed, organic pollutants can be reduced conveniently and efficiently. This high-grade, clean energy technology design may serve as a solution to nonpoint source pollution, livestock-raising pollution, and energy shortages in rural areas, and at the same time it may generate significant environmental and energy benefits (Wang *et al*. 2013). In the major developed countries, biomass energy technology, particularly biogas technology, has been regarded as the most promising accessible renewable energy (Gronowska *et al*. 2009; Kumarappan *et al*. 2009) and has been deemed a viable option for treating vast quantities of wastewater of all kinds (Li *et al*. 2009). As China remains the largest developing country in the world, the successful renewable energy development in China could play a crucial role in energy production and environmental protection worldwide. In recent years, the biogas industry has been growing rapidly in China as one of the most convenient and very accessible popular modes of renewable energy (Wu and Liu 2015), and its technologies have been widely applied in wastewater treatment (Zhang *et al*. 2009). However, in full-scale projects, the remarkable benefits to energy production and environmental protection cannot be seen, and the biogas production rate and pollutant removal rate are both quite low, badly inhibiting the dissemination of the operative technology. One of the principal solutions to this problem is to raise the fermentation efficiency by mixing. Academic studies in various countries have discovered that mixing provides a means of raising the biogas production and pollutant removal rates (McMahon *et al*. 2001). Nevertheless, it has a limited role in promoting the efficiency of anaerobic digestion, and in some biogas plants the digestion efficiency was only slightly promoted after mixing was implemented, as the model limits the potential of fermentation efficiency. Accordingly, the mixing method should be optimized to raise the fermentation efficiency.

Wu *et al.* (2013) suggested that dynamic fermentation, which drives the fermentation slurry flow by external power, is far better than static fermentation, and it was a revolutionary leap in biogas development to promote dynamic fermentation by multiphase flow. Nevertheless, the principal mechanism by which mixing promotes fermentation efficiency remains unclear and may be specific to the method of mixing chosen (Liu *et al*. 2009). Opinions were divided on whether mixing would facilitate the startup period of fermentation or low-concentration fermentation processes. According to Jarvis *et al.* (2005), at the startup of fermentation, biomass turns into flocculating constituents with a weak structure that is likely to be destroyed by the mixing; these structures then become hard during startup. However, Wang *et al.* (2008) pointed out that mixing during the startup period could cut off the loose structures of the flocculating constituents, splitting the dense fraction into smaller particle sizes for better mass transfer. Li (2006) held that the selection of the mixing method should be based on the structural characteristics of the flocculating constituents, while for concentrated fermentation slurry, mixing is a viable method for raising the fermentation efficiency. The higher the total solid (TS) concentration, the more significant an effect the mixing has, but when the TS concentration of the fermentation slurry is lower than 10%, mixing is of little importance (Karim *et al*. 2005). It is worthwhile noting, though, that the digester used for the experiments of Karim was very small, with a volume of only 3 L; bigger digesters were

more dependent on mixing (Bello-Mendoza and Sharratt 1998). Considering the disagreement over the results at different digester sizes, this study conducted analyses and experiments with a 750-L digester, using fully-dissolved, single-phase fluid as the fermentation feedstock (thus, from the aspect of fluid dynamics, a TS concentration of approximately zero) to determine the impact of mixing on the anaerobic digestion of organic wastewater.

This research aimed at uniform mass transfer and even distribution of kinetic energy with a view to optimizing the hydraulic mixing mode in the digester and clarifying the impact of mixing on the anaerobic digestion of low-concentration wastewater. The mechanism of flow fluid optimization and simulation of the flow field were also explored using CDF software for the hydraulic mixing.

EXPERIMENTAL

Anaerobic Digester and Fermentation Material

During the experiment, an anaerobic digester of a 750-L cylindrical tank was used. The main body was a cylindrical tube made of Plexiglas of 800 mm in diameter, 1,330 mm in length, and 12 mm in tube thickness. The tube was bonded with a 15-mm-thick Plexiglas plate at each end. Into the top plate, a 100-mm-diameter hole was drilled to serve as the inlet, and this was connected with an inlet pipe 300 mm in length. During fermentation, when the level of the liquid surface of the influent slurry reached 1,100 mm, which was higher than the bottom end of the inlet pipe, a water seal was formed. As a result, the effective volumes of the fermentation chamber and the biogas storage were 600 L and 150 L, respectively.

An automatic, circulating flow scheme was designed to form an antigravity mixing flow field for the high-position, dispersed pressure outlet. Correspondingly, a fluidized bed can be formed in the digester. A 50-mm-diameter hole was drilled into the center of the bottom plate to serve as the inlet and connected to the outlet of an electronic wastewater pump. Four holes, each with a diameter of 50 mm, were drilled into the tank body, distributed in four directions and located 1000 mm from the bottom plate. These were the outlets of the digester and were connected to four circulating pipes (Part 4 in Fig. 1a). The four circulating pipes were joined into one and connected to the inlet mouth of the wastewater pump, forming the circulating hydraulic passage, in which slurry could circulate from and into the digester by the power of pump.

The overall design of the fermentation device is shown in Fig. 1a. The control test used another two tanks of the same size as the first; one had only one circulating pipe to form the antigravity mixing flow field of the high-position, centralized pressure outlet, while the other had no circulating flow device and was replaced by static fermentation. In the experiment, the digester with four circulating pipes was named 4#, the one with one pipe was named 1#, and the one with no mixing was named 0#; the three digesters are depicted in Fig. 1b. The power of the three digesters was controlled by a frequency converter for regulating the inlet flow rate; the wastewater pump and its frequency converter are shown in Fig. 1c.

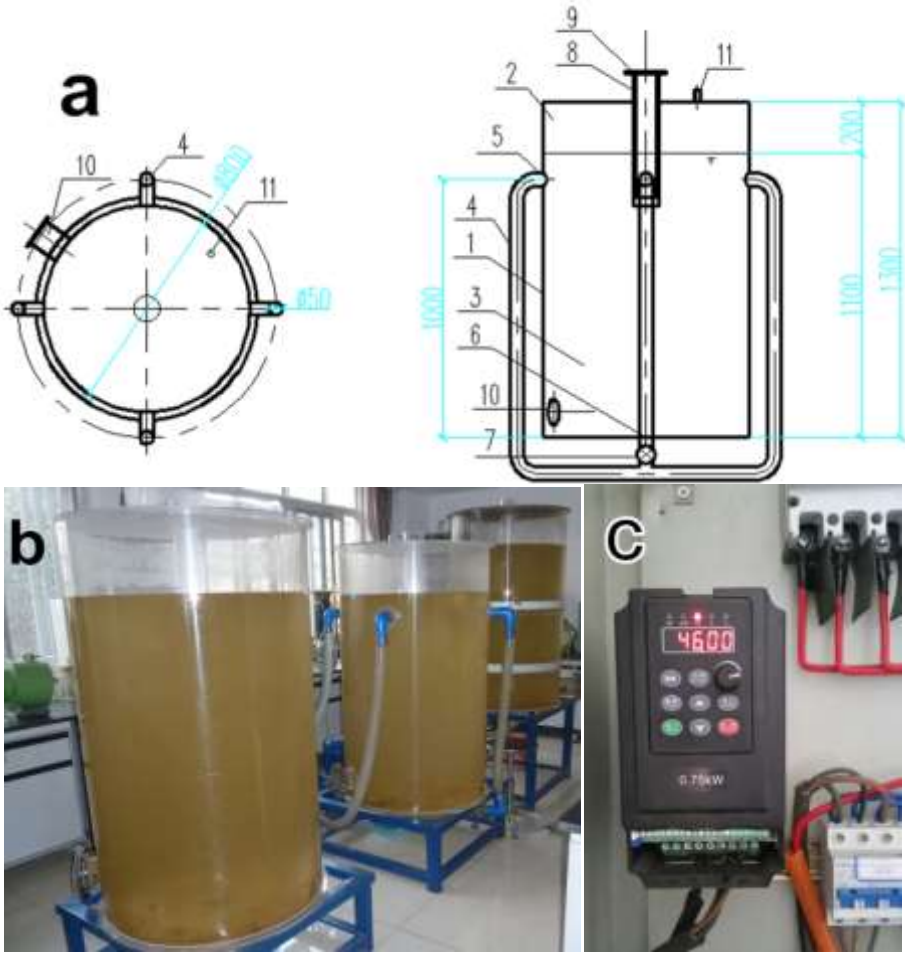

Fig. 1. The employed anaerobic digestion system: a) schematic diagram of the digester with dispersed pressure outlets (1. digester; 2. gas storage chamber; 3. fermentation chamber; 4. liquid pipe; 5. outlet; 6. inlet; 7. pump; 8. inlet whole; 9. seal plug; 10. man hole; 11. gas pipe); b) photos of digesters 1#, 4#, and 0# from left to right; c) AC frequency converter for regulating the power of the pump and adjusting the inlet flow rate

The wastewater from a pharmaceutical factory was taken and prepared as the fermentation feedstock for the experiment. The major product of the pharmaceutical factory is dextran, which is a high-molecular-weight polymer of glucose generated from the fermentation of sucrose by *Leuconostoc mesenteroides*, and its wastewater is typically organic. For the convenient observation of the internal situations of the digesters and the preparation of a fairly realistic condition for the simulation, the wastewater was diluted by mixing it evenly with water to prepare the fermentation feedstock, which could be considered a single-phase liquid. The parameters of the fermentation feedstock are shown in Table 1. In addition, each digester had 3 kg of activated sludge added to enrich the microbes.

Table 1. The Principal Physical Parameters of the Fermentation Feedstock

Density (kg/m³)	Dynamic Viscosity (Pa·S)	pH	COD Concentration (mg/L)	NH3-N Concentration (mg/L)
1.031	0.00325	7.16	28,827	67

Experimental Steps

The experiment was conducted in a laboratory in Chengdu (a temperate city in inland China) from August 7 to September 18, 2014, lasting for 42 days (6 weeks), and the room temperature ranged from 21 °C to 33 °C. The three digesters were tested under the same circumstances: they were simultaneously fed with fermentation feedstock through the top inlet hole until the liquid surface reached 1.1 m, then the seal plug was switched off to start the experiment.

During the experiment, the 0# digester with no mixing was used as the control. In the 1# and 4# digesters, mixing was performed every 4 h (6 times per day), for 15 min each time. The daily biogas production and biogas composition of the three digesters were detected and recorded at the time the mixing was performed. The pH value, COD concentration, and NH_3-N (ammonia nitrogen) concentration, regarded as auxiliary analytical metrics, were tested using a sample of the slurry residue taken through the sampling hole in the digester wall.

The digester wall was made of Plexiglas, which made it convenient to adjust the inlet flow velocity, based on the power setting of the pump, by observing the change in the flow field inside the digester. To determine the inlet flow velocity during mixing, the power of the pump was first set to 0, then raised gradually after it was activated. Consequently, the inlet flow velocity at the bottom of the digester increased slowly, until waves showed up on the liquid surface. This indicated that the principal hydraulic passage at the digester bottom had been formed in the horizontal direction of influent revolving the principal hydraulic passage in the vertical direction, which shows that there was kinetic energy in the dead zone and that the pump power could optimize the inlet flow velocity. However, there was no fluidization at the digester bottom. A slight increase in the flow velocity caused a low-rate vortex at the digester bottom, illustrating the presence of kinetic energy at the dead zone and indicating that the pump power could optimize the inlet flow velocity. During this experiment, the flow velocity at the center of the inlet was measured as 0.7 m/s, with a flow velocity meter, (LS-130A, Tongda Company, China) and this value was used as the boundary condition of the CFD simulation.

Analytical Method

To judge the results of the control tests on the anaerobic fermentation performance of the three digesters, two indices, the biogas production and the physical parameters of the slurry residue, such as pH value, COD concentration, and NH_3-N, were tested. The liquid viscosity coefficient was detected with a rotary viscometer (NXS-11B, Chengdu Instrument Factory, China), the liquid flow velocity was detected with an infrared ray fluid meter (LS-130A, Tongda Company), and both parameters were tested before sealing the digester. There was a sampling hole drilled in the digester wall, through which the slurry in the digester could be sampled to test three metrics: pH value, COD concentration, and NH_3-N concentration. The pH value was tested by the electrode method (Li 2004), the COD value by the potassium dichromate titration method (Yang 1998), and the NH_3-N by ammonia salicylic acid spectrophotometry (Cai *et al*. 2010). These three metrics were tested once every three days, so 15 data points were collected for each metric from each digester during the 42-day experiment. The biogas was extracted through the gas pipe at the top of each digester, the biogas production was monitored with a wet-type flow meter (LML-1, Kesion Electronics, China) for real-time data reading, and the gas composition was analyzed by gas chromatography (Li *et al*. 2015).

RESULTS AND DISCUSSION

Biogas Production Index

The biogas production is a basic measure of the biogas fermentation efficiency. The parallel experiments indicated that the varied mixing methods had different impacts on fermentation efficiency. Figure 2 shows the comparison of the biogas production indices.

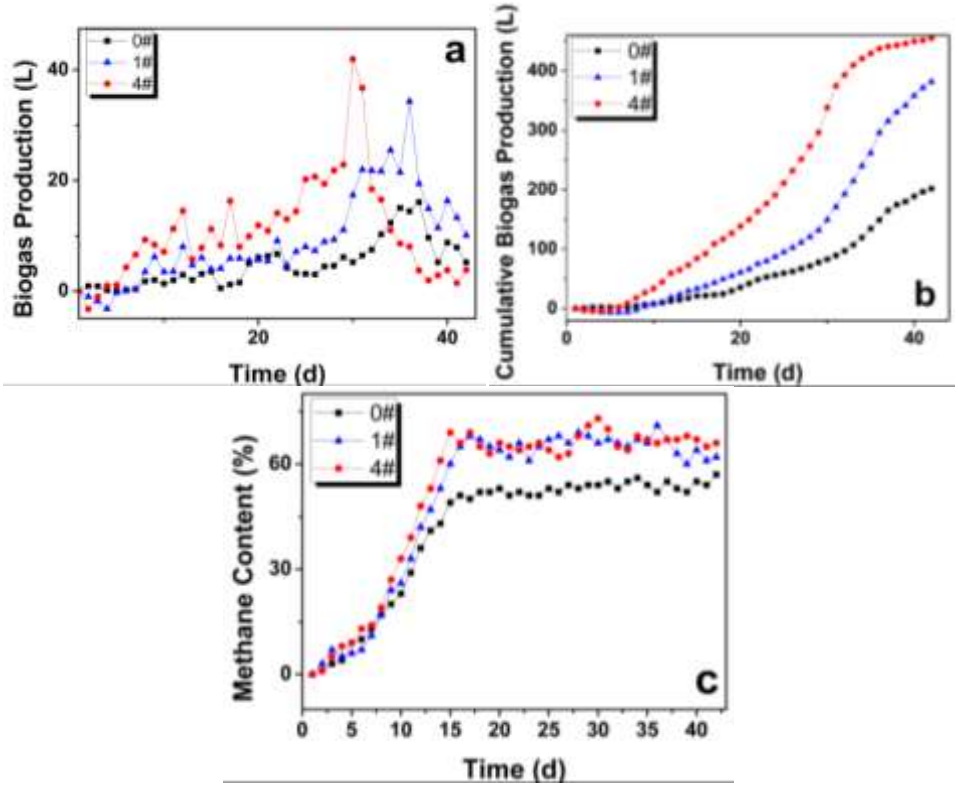

Fig. 2. Comparison of the biogas production indices: a) daily biogas production; b) cumulative biogas production; c) methane content in biogas

Figure 2a shows that 4# was the first digester to begin normal biogas production, immediately followed by 0#, and 1# was the last to begin. Clearly, the startup was abnormal if there was no mixing or uneven mixing. Based on the fact that 1# reached the biogas production peak earlier than 0#, even uneven mixing could visibly raise the fermentation efficiency during normal biogas production. The 1# digester reached a biogas production peak on day 36, and the 4# digester peaked on day 30, periods that were 1 d and 7 d earlier than the 0# digester, respectively.

When the feedstock in 4# became fully decomposed, on day 30, its daily biogas production rate became lower than that of 1#. From Fig. 2b, the gap in cumulative biogas production between the two digesters started to narrow on day 30, though the two never reached equal levels. From Fig. 2c, the methane content in the three digesters reached a steady value on day 15, and the methane content of 1# and 4# were far higher than that of 0#, with a slight gap between 1# and 4#.

Comprehensive Biogas Production Index

At the end of the experiment on day 42, the daily biogas production of the three digesters had dropped below 5 L/d, indicating the exhaustion of the feedstock. The comprehensive biogas production index is shown in Table 2. The average daily biogas production of 1# was 89% higher than that of 0#, and that of 4# was 125% higher than that of 0#.

Table 2. Biogas Production of the Anaerobic Fermentation Process and the Removal Rate of Pollutants on Day 42

Digester	Daily Biogas Production (L/d)	Cumulative Biogas Production (L)	Average Methane Content (%)	COD Biogas Production Rate (L/kg COD)	COD Removal Rate (%)
0#	4.80	201.77	41.24	13.31	52.60
1#	9.08	381.60	50.17	19.81	66.83
4#	10.83	455.05	52.12	21.07	74.93

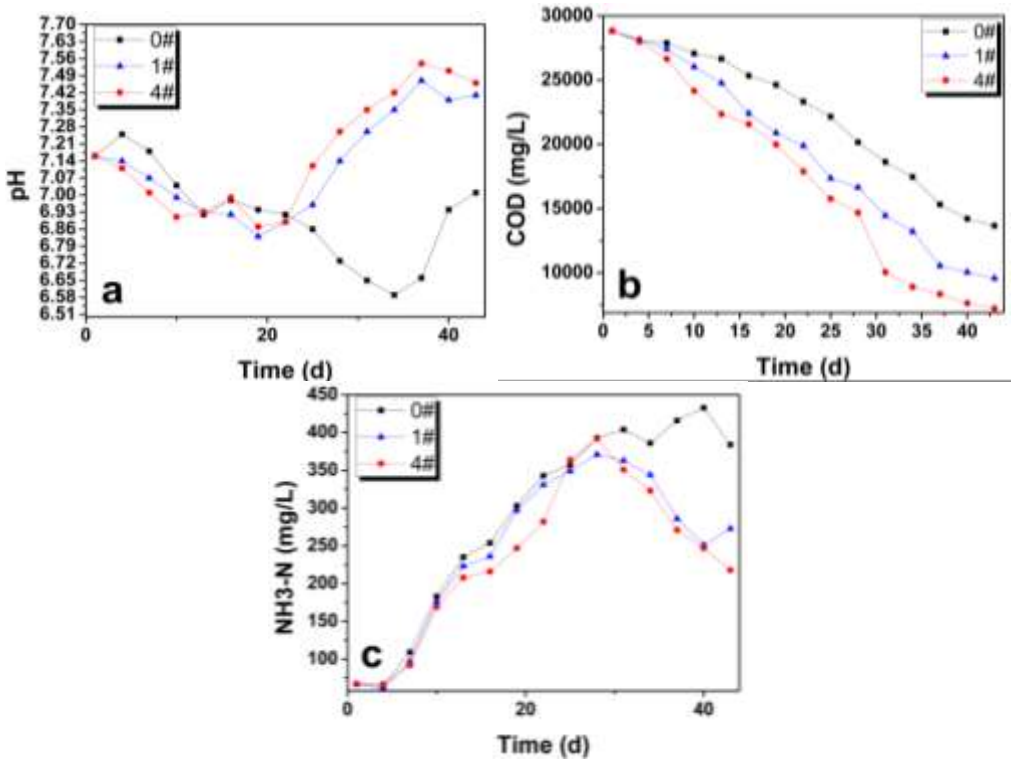

Fig. 3. Variation in the physical properties of the fermentation slurry: a) pH variation; b) variation in COD concentration; c) variation in ammonia nitrogen concentration

Figure 3a shows that, in the initial period of the experiment, the acidification of 4# proceeded in the shortest time, followed by that of 1#, then 0#. This sequence indicated that mixing could shorten the hydrolysis phase of the slurry and hasten the acidification. On day 18, the acidification was inhibited in 4# and 1#, simultaneously, so the pH began to rise and was maintained at around 7.4, a weakly-alkaline environment suitable for biogas fermentation. In 0#, the acidification was not inhibited until day 33, when the pH dropped below 6.4, then rose back to around 6.8, a slightly acidic value. If there had been no mixing, the hydrolysis phase would have been longer, acidification would have started later, and

the acidity would have been higher in the acidification phase. Thus, mixing could inhibit the acidification of the slurry, raise the buffering capacity of the fermentation system, and create a weak alkaline environment more suitable for biogas anaerobic fermentation.

Figure 3b shows the variation in the COD concentration of the slurry for the three fermentation systems. The COD declined the slowest in 0#, while 1# and 4# were faster, comparatively, despite the narrow gap between the two. The COD decreased in 1# and 4# at rates 27% and 42% greater than that of 0#, respectively. Consequently, mixing could accelerate the degradation of COD in the slurry and enhance the digestion efficiency.

Figure 3c shows the variation in the concentration of ammonia from the nitrogen residue of the feedstock in the three digesters; the initial NH_3-N across all three digesters was as low as 67 mg/L and rose rapidly during fermentation. The gap between the NH_3-N of 0# and 1# was narrow, and both were higher than that of 4#. On day 27, the values of 1# and 4# began to drop, while that of 0# dropped on day 36. The NH_3-N of the three digesters coincided with the biogas production peaks, indicating that the anaerobes used NH_3-N as a nutrient were able to facilitate digestion (He *et al*. 2005), leading to the biogas production peak. Thus, mixing was beneficial not only for the reduction of NH_3-N formation in the solution, but also for the digestion of NH_3-N by anaerobes.

From the comparison of the principal indices, including biogas production efficiency, pH value, COD concentration, and NH_3-N concentration, during biogas fermentation, mixing had no advantage over non-mixing with regards to biogas production efficiency and pollutant removal effect. The mixing obtained using the high-position, dispersed pressure outlet was better than that of the high-position, centralized pressure outlet, as evidenced by the flow field form of the former mixing method; this phenomenon could be explained by CFD numerical simulation to some extent.

CFD Numerical Simulation

The actual form of the flow field in the slurry was difficult to observe and record, but it could be visually approximated by numerical simulation with fluid mechanics software, the precision of which has been well tested (Vesvikar and Al-Dahhan 2005; Shen *et al*. 2013). It was particularly suitable for the flow field simulation of reactors with hydraulic mixing (Wang *et al*. 2010). Using the CFD method, this work simulated calculations for the two designs, the high-position, centralized pressure outlet and the high-position, dispersed pressure outlet, and determined the difference in their flow fields visually.

Simulation Objects and Conditions

The recycling tube had a small volume and was not the principal fermentation area, while the gas storage chamber was only used to store biogas and had no impact on fermentation; therefore, they were both ignored in the simplified model. The simplified model, with only a fermentation chamber, was a 600-L liquid column with an opening in the bottom as the velocity inlet, and the openings in the side wall were used as pressure outlets.

The two digesters were built with grids, and the grids were divided by the control volume method, with 1,000 grids on each side. The model of 1# produced 3,302,332 grids, and the model of 4# produced 3,295,462 grids, as shown in Fig. 4.

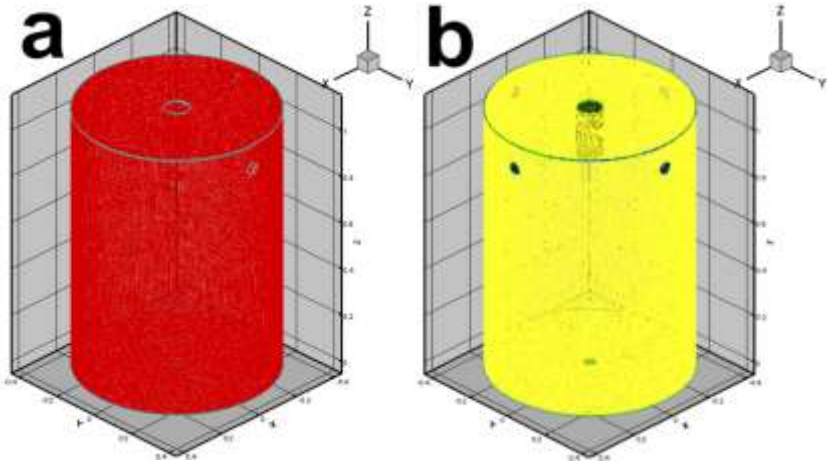

Fig. 4. Grid model of the digesters: a) numerical model of 1#; b) numerical model of 4#

Numerical Calculation Method

As the fermentation slurry was extremely soluble in water and had a low solid activated sludge content, the medium in the simulation could be assumed to be a single-phase liquid. The continuity equation of the fluid flow is shown below (Eqs. 1 through 5):

$$\frac{\partial(\rho u_x)}{\partial x}+\frac{\partial(\rho u_y)}{\partial y}+\frac{\partial(\rho u_z)}{\partial z}=0 \quad (1)$$

From this relationship, a series of dynamic equations was formulated:

$$\nabla\cdot(\rho u_x\vec{u}) = -\frac{\partial\rho}{\partial x}+\frac{\partial\tau_{xx}}{\partial x}+\frac{\partial\tau_{xx}}{\partial y}+\frac{\partial\tau_{xx}}{\partial z}+\rho f_x \quad (2)$$

$$\nabla\cdot(\rho u_y\vec{u}) = -\frac{\partial\rho}{\partial y}+\frac{\partial\tau_{xy}}{\partial x}+\frac{\partial\tau_{yy}}{\partial y}+\frac{\partial\tau_{zy}}{\partial z}+\rho f_y \quad (3)$$

$$\nabla\cdot(\rho u_z\vec{u}) = -\frac{\partial\rho}{\partial z}+\frac{\partial\tau_{xz}}{\partial x}+\frac{\partial\tau_{yz}}{\partial y}+\frac{\partial\tau_{zz}}{\partial z}+\rho f_z \quad (4)$$

In these equations, ∇ is the Hamiltonian differential operator:

$$\nabla = i\frac{\partial}{\partial x}+j\frac{\partial}{\partial y}+k\frac{\partial}{\partial z} \quad (5)$$

Simulation Results of the Flow Pattern

In the experiments, the inlet flow velocity was taken to be 0.7 m/s, and this value was used as the boundary condition for the simulation. From the simulation, there was a vast gap in the flow fields of 1# and 4#.

Figure 5a shows the comparison of the velocity vector distribution between model 1# and model 4#. Figures 5b and c display the comparison of the plane cross section diagrams between the two digesters at heights of 1 m and 0.1 m, respectively. Figure 5d indicates the velocity vector distribution of model 4# with an inlet flow velocity boundary condition of 2 m/s.

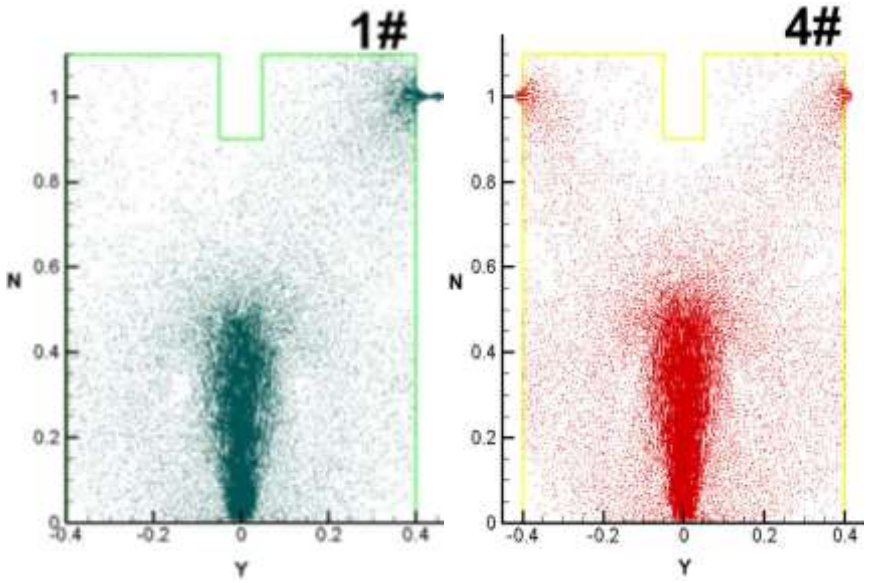

a) v = 0.7 m/s, velocity vector diagrams of section x = 0

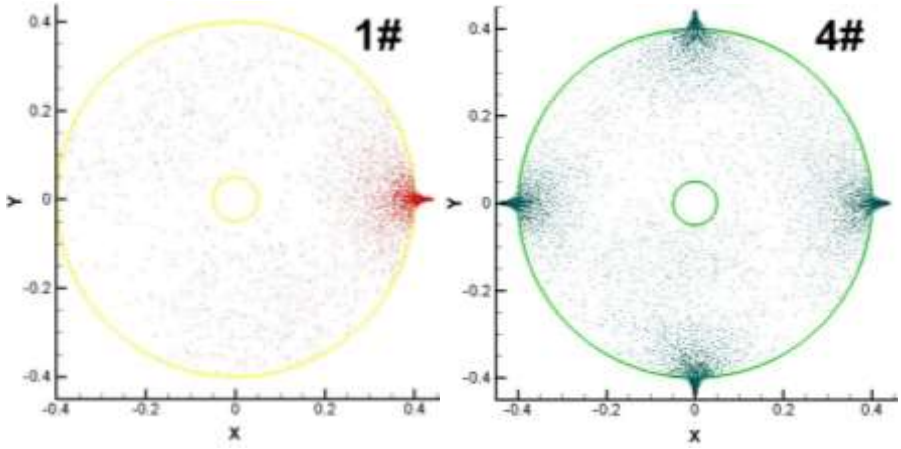

b) v = 0.7 m/s, velocity vector diagrams of section z = 1

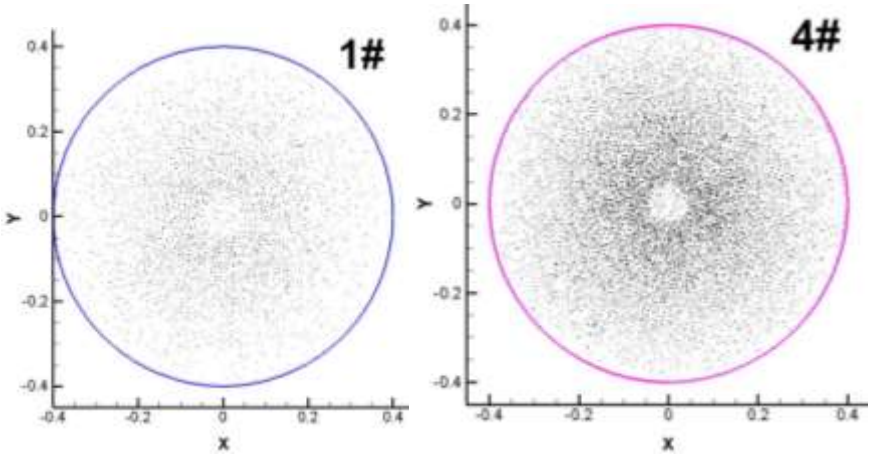

c) v = 0.7 m/s, velocity vector diagrams of section z = 0.1

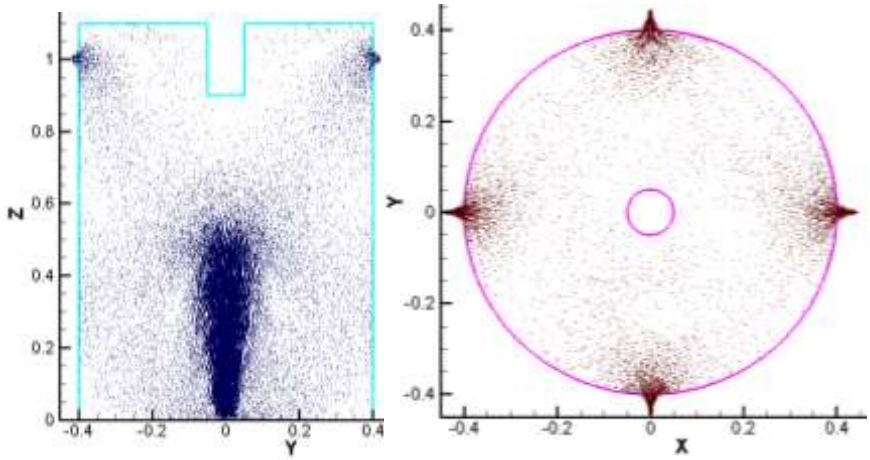

d) v = 2 m/s, velocity vector diagrams of section x = 0 and section z = 1 of model 4#

Fig. 5. Comparison of the section drawings of the simulative flow fields

From the CFD simulation, the flow fields of model 1# and model 4# were found to have huge differences. Figure 5a shows the velocity vector distributions of the two models at an inlet velocity of 0.7 m/s. The figure demonstrates that the kinetic energies were plentiful, but the kinetic energy distribution was uneven in 1#, as it was rich at the side with the outlets and seriously deficient on the other side. However, in 4#, the kinetic energy was distributed evenly in all four directions, owing to the symmetrical placement of the pressure outlets at the high positions, leaving no areas deficient in kinetic energy. Figure 5b shows the plane cross section diagrams of the 1# and 4# digesters at the level of the outlet, 1 m high, which was also the high position of the digester. This figure shows more clearly the difference between the two models, as a high amount of kinetic energy gathered on the side with no outlet. Since other areas were relatively stagnant by comparison, the kinetic energy distribution of 4# was relatively even. Figure 5c shows the plane cross section diagrams of the 1# and 4# digesters at the low position, 0.1 m high, at an inlet flow velocity of 0.7 m/s. At the low position of the digester, the kinetic energy distribution of 1# was uneven and worse than that of 4#, even on the outlet side; correspondingly, the vortex was even weaker at the low position during the experiments. It has been noted that the design of 4#, compared to that of 1#, was easier to form a balanced flow field in large digesters and an even distribution of the kinetic energy in large areas of the digester.

In Fig. 5d, the velocity vector distribution diagram of 4# indicates that the form of the flow field in 4# had no obvious changes, despite increasing the inlet flow velocity to 2 m/s. This phenomenon indicated that continued increases in the inlet flow velocity could not further optimize the flow form, so 0.7 m/s was deemed the most suitable inlet velocity.

The Effect of Mixing on Biogas Production Efficiency

A comparison of the biogas production rates among the three digesters further confirmed the view that mixing was beneficial in raising the biogas production efficiency: the biogas production rates in the digesters with mixing, 1# and 4#, were 89% and 125% higher, respectively, than that with no mixing. In this study, a low-concentration slurry was used as the fermentation feedstock, with a TS concentration near 0, but, nevertheless, the effect of mixing was distinctive. The two different mixing methods had considerably different impacts on the increase in biogas production, which was much higher in 4# than in 1#. This result indicated that optimized design of the flow field could produce a more

even flow field form and play a remarkable role in increasing the mixing efficiency. The biogas production peaks of the two digesters with mixing appeared 1 d and 7 d earlier than that of the digester with no mixing, indicating that mixing was beneficial for a quicker startup of the anaerobic fermentation, and the impact was more notable with balanced mixing, as in the 4# digester.

The increase in the biogas production efficiency resulted from the optimization of the mixing flow field form. Mixing can transform static fermentation into dynamic fermentation, facilitate the even distribution of kinetic energy in the fermentation area, and create formations that inhibit dead zones (Wu and Chen 2011). Due to gravity, the kinetic energy distribution increased in the vertical direction, but anti-gravity mixing could be conducted to resist this trend (Huang *et al*. 2014). While stratification in the fermentation slurry was unavoidable, it could be reduced through the hydraulic passage throughout the digester (Huang *et al*. 2014). Accordingly, in this experiment, the reactor built for circulation fluidization was designed with inlets at the bottom and outlets at a high position. Based on the CFD simulation, this design could counter gravity and form a complete hydraulic passage in the middle of the digester, from the bottom to the top.

There was only one outlet at the high position of 1#, so, though circulating fluidization could be formed, the massive kinetic energy increases on the outlet side resulted in an imbalanced flow field. As the microbes and scarce elements could not be transported to the stagnant areas, a vast fermentation blind area was formed. In 4#, the outlets placed symmetrically in four directions in the digester wall facilitated the even distribution of the flow field in both the horizontal and vertical directions. As a result, there were no obvious stagnant areas, and the microbes and scarce elements could be distributed evenly across the fermentation area, enlarging the effective fermentation volume and raising the biogas production efficiency.

The 1# and 4# digesters were quite similar in methane content, and both were much higher than 0#. The circulating fluidization mixing method could raise the methane content in the biogas more than by optimizing the form of the flow field, which generated only a slight increase in the methane content. This discrepancy is probably explained by the large quantity of acidic byproducts formed during anaerobic fermentation, which are highly inhibitive to the methanogens and cause a reduction in methane production, the generation of redundant CO_2, and a decrease in methane content (Zhou *et al*. 2002). In the fermentation area, the localized acidification could be expanded by dissolution, so timely mixing was essential for reducing the acidity. As Fig. 3a shows, the acidity of 0# was initially low, and its pH value was higher than those of 1# and 4# due to its low fermentation velocity and acid production. With the accumulation of acidic substances, the acidity of 0# rose continuously, while the acidifications of 1# and 4# were restrained until around day 20 due to mixing. On day 25, the pH value rose to, and exceeded, 7.0, and the biogas production peak appeared. The acidity of 1# was slightly higher than that of 4# and, accordingly, its methane content was a bit lower than that of 4#. This result showed that the stagnant area was conserved by imbalanced mixing, and the maintaining of conditions conducive to the accumulation of acidic substances in a small area caused the pH drop. The acidic substances were highly soluble in water and could be rapidly dissolved even with light mixing, though 1# had a weak flow field form that caused a kinetic energy shortage in many areas and allowed for sufficient acidification inhibition. Therefore, the effect of the flow field form of 1# on the acidification inhibition had no obvious difference from that of 4#. The results suggested that as long as back-flow was formed, acidification could be

inhibited, and the optimized flow field form had no obvious beneficial impact on acidification inhibition.

Impact of Mixing on Pollutant Removal Rate

Pollutant removal was another significant goal of this experiment, besides biogas production. In this study, pharmaceutical wastewater was used as the fermentation feedstock, and the principal pollutant metrics were COD and NH_3-N. As Fig. 3b shows, during fermentation, 4# had the fastest COD degradation, followed by 1# and 0#, in sequence. In addition, there was no obvious drop on day 25, indicating that the anaerobic fermentation had been heavily weakened. This phenomenon could be explained by the fact that the activated sludge, rich in methanogens, settled on the bottom of the digester, prohibiting mass contact between the fermentation slurry and the bacteria in the fermentation area and forming a dead zone of static fermentation (Jia *et al*. 2015). It could also be due to the sedimentation of scarce auxiliary elements, such as phosphorus (P), potassium (K), sulfur (S), iron (Fe), cobalt (Co), and nickel (Ni), which are indispensable for the anaerobic fermentation reaction in the digester (Li *et al.* 2014; Huang *et al.* 2015; Zhao *et al.* 2015). These elements in the slurry were low in content, high in density, and easy to settle, and its dead zone was larger than that of the activated sludge. By antigravity mixing, the scarce elements in 1# and 4# surged from the bottom to the high position of the digester, and the activated sludge and scarce elements were pushed by the fluid to areas that could be reached by the kinetic energy generated by the hydraulic mixing. Using dynamic fermentation, dead zones of static fermentation would not be formed, and the fermentation efficiency could then be raised.

The above situation was not witnessed in the experiments using small digesters, as, under low hydraulic pressure, activated sludge and scarce elements could rapidly fill the extremely small space simply by dissolution diffusion, rather than a dependence on external forces. In the large digesters used in this work, the liquid columns were higher than 1 m, and, when the activated sludge settled to a low position, it was under extremely high pressure, making it difficult to diffuse to a large space; thus, external force was indispensable for mixing. To some extent, this experiment resolved the different views of Karim (2005) and Bello-Mendoza (1998) on whether mixing was a necessity for low-concentration fermentation.

Unlike the continuous decrease of COD in anaerobic fermentation, the accumulation and conversion of NH_3-N occurred simultaneously, with a complicated variation. Hansen *et al.* (1998) built a four-phase model of NH_3-N accumulation in anaerobic fermentation:

$$\text{Stage 1:} \quad 0 < [NH_3] < 1.10, \mu_r = 1.0$$
$$\text{Stage 2:} \quad 1.10 < [NH_3] < 1.16, \mu_r = \frac{1}{-7.6+\frac{[NH_3]}{0.128}}$$
$$\text{Stage 3:} \quad 1.16 < [NH_3] < 1.34, \mu_r = 0.67$$
$$\text{Stage 4:} \quad 1.34 < [NH_3], \quad \mu_r = \frac{1}{-12+\frac{[NH_3]}{0.0995}}$$

NH_3-N is the nutrient source for the anaerobes at the low-concentration stage and provides indispensable alkalinity to the fermentation system, but an excessive NH_3-N concentration is toxic to the reproduction of methanogens. However, according to Zhang *et al.* (2003), the toxicity of NH_3-N is reversible, and its accumulation can be restrained to

relieve the toxicity by methods such as dilution and mixing. In this experiment, the initial NH_3-N concentration of the fermentation feedstock was fairly low, only 67 mg/L, based on the monitored NH_3-N data in the three digesters shown in Fig. 3 (C). During the initial fermentation period, a slight accumulation of NH_3-N occurred in the three digesters, at similar rates. After about 25 days, the accumulation rates of NH_3-N in the two digesters with mixing were slightly lower than that of the digester with no mixing, and the rates were restrained on day 28, which was the beginning of the NH_3-N drop. The biogas production peak appeared at this time, indicating that mixing was beneficial for NH_3-N conversion, NH_3-N accumulation inhibition, reproduction of bacteria, and biogas production. The NH_3-N concentrations of 1# and 4# were quite close, indicating that, similar to the pH value, back-flow mixing, once formed, could be beneficial for NH_3-N conversion and NH_3-N accumulation inhibition, while optimizing the flow field form had no obvious impact on the inhibition of NH_3-N accumulation.

CONCLUSIONS

1. Anti-gravity mixing is a novel, effective circulating fluidization method in which the high-position, dispersed pressure outlets can optimize the flow pattern into an even form, eliminate the areas which are deficient in kinetic energy, and noticeably promote biogas production and the COD removal rate.
2. Through comparative experiments on the anaerobic fermentation of organic wastewater in a 750-L digester, this work has illustrated that, in large digesters, mixing had a significant impact on the promotion of biogas production and pollutant removal during the anaerobic fermentation of low-TS-concentration slurry.
3. An optimized flow pattern can raise biogas production and the COD removal rate, but it cannot help much in inhibiting acidification, facilitating NH_3-N conversion, inhibiting NH_3-N accumulation, or raising the methane content. As long as circulating fluidization is maintained, the capacities of acidification inhibition, inhibition of NH_3-N accumulation, and methane content rise are relatively small.

ACKNOWLEDGMENTS

The authors gratefully acknowledge the financial support of the National Nature Science Foundation of China, under Grant Nos. 51478280 and 51178282, and the Agricultural Science and Technology Innovation Program (ASTIP), P.C. China.

REFERENCES CITED

Bello-Mendoza, R., and Sharratt, P. N. (1998). "Modelling the effects of imperfect mixing on the performance of anaerobic reactors for sewage sludge treatment," *Journal of Chemical Technology and Biotechnology* 71(8), 121-130. DOI: 10.1002/(SICI)1097-4660(199802)71:2<121::AID-JCTB836>3.0.CO;2-7

Cai, L., Chen, T. B., Liu, H.T., Gao, D., Zheng, G. D., and Zhang, J. (2010). "Time domain reflectometry measured moisture content of sewage sludge compost across temperatures," *Waste Manage*. 33(1), 12-17

Gronowska, M., Joshi, S., and MacLean, H. L. (2009). "A review of U.S. and Canadian biomass supply studies," *BioResources* 4(1), 341-369. DOI: 10.15376/biores.1.1.1-2

Hansen, K., Angelidaki, I., and Ahring, B. (1998). "Anaerobic digestion of swine manure: inhibition by ammonia," *Water Research* 32(1), 5-12. DOI: 10.1016/S0043-1354(97)00201-7

He, S., Wang, J., and Zhao, X. (2005). "Effect of ammonium concentration on the methanogenic activity of anaerobic granular sludge," *Journal of Tsinghua University (Science and Technology)* 45(9), 1294-1296. DOI: 1000.0054(2005)09.1294.03

Huang, L., Tao, H., Su, Y., Zhang, W., Tang, Y., Yang, Y., Liu, H. (2015). "The study of the effect of metal ion on biogas anaerobic fermentation and desulfurization," *Renewable Energy Resources* 33(3), 448-451. DOI:10.13941/j.cnki.21-1469/tk.2015.03.019

Huang, R., Long, Y., Luo, T., Mei, Z., Wang, J., and Long, E. (2014). "The research on optimization of the multiphase flow field of biogas plant by using CFD software," *Journal of Energy and Power Engineering* 8(1), 1038-1046.

Jarvis, P., Jefferson, B., Gregory, J., and Parson, S. A. (2005). "A review of floc strength and breakage," *Water Research* 39(14), 3121-3137. DOI: 10.1016/j.watres.2005.05.022

Jia, L., Yu, F., Ning, P., Xiong, X., Wang, H., Liu, T., Wang, B. (2015). "Influence of temperature, concentration of substrate and trace elements on anaerobic fermentation with dairy manure," *Transactions of the Chinese Society of Agricultural Engineering* 30(22), 260-266. DOI: 10.3969/j.issn.1002-6819.2014.22.032

Karim, K., Hoffmann, R., Klasson, T., and Al-Dahhan, M. H. (2005). "Anaerobic digestion of animal waste: Waste strength versus impact of mixing," *Bioresource Technology* 96(4), 1771-1781. DOI: 10.1016/j.biortech.2005.01.020

Kumarappan, S., Joshi, S., and MacLean, H. L. (2009). "Biomass supply for biofuel production: Estimates for the United States and Canada," *BioResources* 4(3), 1071-1087.

Li, J., Wei, L., Duan, Q., Hu, G., and Zhang, G. (2014). "Semi-continuous anaerobic co-digestion of dairy manure with three crop residues for biogas production," *Bioresource Technology* 156(1), 307–313. DOI: 10.1016/j.biortech.2014.01.064

Li, J., Zhang, Y., Li, W., Lv, J. (2015). "Study on biogas content by gas chromatography," *Agricultural Mechanization Research* 6(1), 307-313. DOI: 10.13427/j.cnki.njyi.2015.06.062

Li, R., Chen, S., Li, X., Lar, J. S., He, Y., and Zhu, B. (2009). "Anaerobic codigestion of kitchen waste with cattle manure for biogas production," *Energy & Fuels* 23(4), 2225-2228. DOI: 10.1021/ef8008772

Li, T., Zhu, Z., Wang, D., and Yao, C. (2006). "Characterization of floc size, strength and structure under various coagulation mechanisms," *Power Technology* 168(2), 104-110. DOI: 10.1016/j.powtec.2006.07.003

Li, W. (2004). "Simple pH meter," *Industrial Water Treatment* 24(11), 61-62.

Liu, Y., Wang, Z., Kong, C., and Deng, L. (2009). "Research progress of mixing and stirring process in biogas fermentation," *China Biogas* 27(3), 26-30. DOI: 10.3969/j.issn.1000-1166.2009.03.006

McMahon, K. D., Stroot, P. G., Mackie, R. I., and Raskin, L. (2001). "Anaerobic co-digestion of municipal solid waste and biosolids under various mixing conditions - II: microbial population dynamics," *Water Research* 35(7), 1817-1827. DOI: 10.1016/S0043-1354(00)00438-3

Shen, F., Tian, L., Yuan, H., Pang, Y., Chen, S., Zou, D., Zhu, B., Liu, Y., and Li, X. (2013). "Improving the mixing performances of rice straw anaerobic digestion for higher biogas production by computational fluid dynamics (CFD) simulation," *Applied Biochemistry and Biotechnology* 171(3), 626-642. DOI: 10.1007/s12010-013-0375-z

Vesvikar, M. S., and Al-Dahhan, M. (2005). "Flow pattern visualization in a mimic anaerobic digester using CFD," *Biotechnology and Bioengineering* 89(6), 719-732. DOI: 10.1002/bit.20388

Wang, M., Li, W., Liu, S., Liu, D., Yin, L., and Yuan, H. (2013). "Biogas production from Chinese herb-extraction residues: Influence of biomass composition on methane output," *BioResources* 8(3), 3732-3740. DOI: 10.15376/biores.8.3.3732-3740

Wang, X., Ding, J., Guo, W., and Ren, N. (2010). "A hydrodynamics-reaction kinetics coupled model for evaluating bioreactors derived from CFD simulation," *Bioresource Technology* 101(24), 9749-9757. DOI: 10.1016/j.biortech.2010.07.115

Wang, Y., Wang, Q., Wu, Y., An, Y., and Peng, X. (2008). "Morphological characteristics of algae floc and its relation with flotation," *Environmental Science* 29(3), 688-695. DOI: 0250-3301 (2008) 03-0688-08. DOI: 10.3321/j.issn:0250-3301.2008.03.025

Wu, B., and Chen, Z. (2011). "An integrated physical and biological model for anaerobic lagoons," *Bioresource Technology* 102(8), 5032-5038. DOI: 10.1016/j.biortech.2011.01.076

Wu, J., and Liu, Y. (2015). "Construction of circular agriculture mode with core of methane," *Agricultural Engineering* 5(1), 26-27.

Wu, M., Liu, T., Yi, Q., Xiang, Y., Zuo, X., Chen, Z., Li, Y., and Li, C. (2013). "Continuous dynamic fermentation in the application of scale piggery wastewater," *Hunan Animal Science and Veterinary Medicine* 173(1), 11-13. DOI: 10.3969/j.issn.1006-4907.2013.01.005

Yang, X. (1998). "Quick determination of COD by potassium dichromate method," *Yunnan Environment Science* 17(1), 61-63. DOI:10.13623/j.cnki.hkdk.1998.01.019.

Yu, F., and Wu, J. (2008). "Toxicity study of ammonium on methanogenic bacteria in anaerobic granular sludge," *Chemistry & Bioengineering* 25(4), 75-78. DOI: 10.3969/j.issn.1672-5425.2008.04.021

Zhang, B., Xu, J., and Cai, W. (2003). "Review on the ammonia inhibition for anaerobic digestion," *China Biogas* 21(3), 26-31. DOI: 10.3969/j.issn.1000-1166.2003.03.007

Zhang, L., Yang, Z., Chen, B., and Chen, G. (2009). "Rural energy in China: Pattern and policy," *Renewable Energy* 34(12), 2813-2823. DOI: 10.1016/j.renene.2009.04.006

Zhao, L., Tian, M., Li, X., Shi, X. (2015). "Influence of trace elements to anaerobic fermentation of corn stalk on biogas production and enzymic F420 activity," *Agricultural Mechanization Research* 6(1), 251-254. DOI: 10.13427/j.cnki.njyi.2015.06.061

Zhou, H., Chen, J., Zhao, Y., and Zhou, Q. (2002). "Methanogenic activity of anaerobic granular sludge by long-chain fatty acids," *Technology of Water Treatment* 28(2), 93-97. DOI: 10.3969/j.issn.1000-3770.2002.02.009

Article submitted: March 13, 2015; Peer review completed: May 15, 2015; Revisions accepted: June 11, 2015; Published: June 17, 2015.
DOI: 10.15376/biores.10.3.4826-4842